ELSEVIER

Bioelectrochemistry 52 (2000) 203–211

Bioelectrochemistry

www.elsevier.com/locate/bioelechem

Torocyte shapes of red blood cell daughter vesicles

Aleš Iglič [a,*], Veronika Kralj-Iglič [b], Bojan Božič [b], Malgorzata Bobrowska-Hägerstrand [c], Boris Isomaa [c], Henry Hägerstrand [c]

[a] *Laboratory of Applied Physics, Faculty of Electrical Engineering, University of Ljubljana, Tržaška 25, SI-1000 Ljubljana, Slovenia*
[b] *Institute of Biophysics, Faculty of Medicine, University of Ljubljana, SI-1000 Ljubljana, Slovenia*
[c] *Department of Biology, Åbo Akademi University, FIN-20520, Åbo Turku, Finland*

Received 8 November 1999; received in revised form 15 March 2000; accepted 18 March 2000

Abstract

The shape of the newly described torocyte red blood cell endovesicles induced by octaethyleneglycol dodecylether (C12E8) is characterized. A possible explanation for the origin and stability of the observed torocyte endovesicles is suggested. Three partly complementary mechanisms are outlined, all originating from the interaction of C12E8 molecules with the membrane. The first is a preferential intercalation of the C12E8 molecule into the inner membrane layer, resulting in a membrane invagination which may finally close, forming an inside-out endovesicle. The second is a preference of the C12E8-induced membrane inclusions (clusters) for small local curvature which would favour torocyte endovesicle shape with large regions of small or even negative membrane mean curvatures, the C12E8 membrane inclusion being defined as a complex composed of the embedded C12E8 molecule and some adjacent phospholipid molecules which are significantly distorted due to the presence of the embedded C12E8 molecule. The preference of the C12E8 inclusions for zero or negative local curvature may also lead to the nonhomogeneous lateral distribution of the C12E8 inclusions resulting in their accumulation in the membrane of torocyte endovesicles. The third possible mechanism is orientational ordering of the C12E8-induced inclusions in the regions of torocyte endovesicles with high local membrane curvature deviator.

Keywords: Membrane; Phospholipid; C12E8 molecule; Curvature deviator; Anisotropic membrane inclusion

1. Introduction

By intercalating preferentially into one of the membrane bilayer leaflets, amphiphilic molecules may significantly change the erythrocyte shape [1–4]. We have recently reported that octaethyleneglycol dodecylether(CH_3-$(CH_2)_{11}(OCH_2CH_2)_8OH$) (Fig. 1a) may induce in erythrocytes (usually one) stable endovesicle having a torocyte shape [5]. The octaethyleneglycol dodecylether (C12E8)-induced torocyte endovesicle consists of a compressed plate-like central region and a toroidal periphery (Fig. 2). It was observed that the torocyte endovesicle originates from a primary large stomatocytic invagination which upon continuous intercalation of the C12E8 molecules into the membrane loses volume. The invagination may finally close, forming an inside-out endovesicle with small relative volume (v), i.e. with large surface area (A) and small enclosed volume (V).

At the present state of the development of the mathematical models for determination of the cell shape, it is not possible to describe the whole transformation of the initially normal discoid erythrocyte shape into the final rounded shape containing the torocyte endovesicle. Our study is, therefore, limited to the analysis of the final shape of the torocyte endovesicle.

The phase diagram of stable shapes of vesicles with no internal structure has been extensively studied [6–9]. However, aside from an early work of Deuling and Helfrich [6], the class of the torocyte shapes was not given attention. Therefore, it is of interest to understand general as well as specific mechanisms that take place in the C12E8-induced torocyte endovesiculation.

In the previous work [5], the possible explanations of the formation of the torocyte endovesicle shape were

* Corresponding author. Tel.: +386-1-250-278; fax: +386-1-1264-630.
E-mail address: ales.iglic@fe.uni-lj.si (A. Iglič).

0302-4598/00/$ - see front matter
PII: S0302-4598(00)00103-3

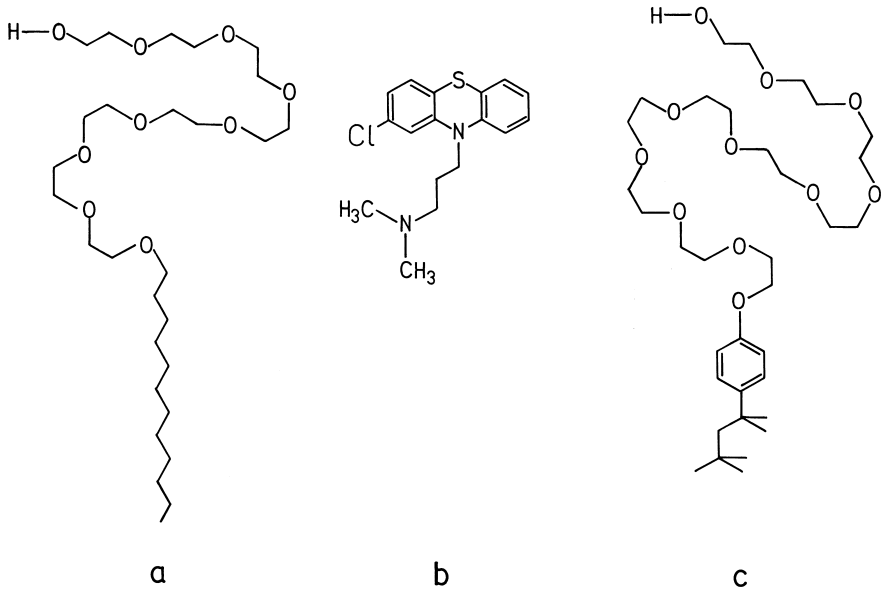

Fig. 1. Schematic illustration of the chemical structure of three different amphiphilic molecules:(a) octaethyleneglycol dodecylether, (b) chlorpromazine and (c) Triton X-100.

briefly indicated. In the present work, we present in detail specific effects of C12E8 molecules within the theory based on the interaction between the C12E8 molecule and the membrane. The molecular features of C12E8 are compared to the molecular features of stomatocytogenic amphiphiles chlorpromazine (Fig. 1b) and Triton X-100 (Fig. 1c) which induce small spherical endovesicles in erythrocytes [5]. A possible region in the geometrical phase diagram belonging to the class of the axisymmetrical torocyte endovesicle shapes with equatorial mirror symmetry is investigated.

2. Geometrical characterization of the class of the torocyte shapes within the bilayer couple model

Within the bilayer couple model [2,7,10,11], the cell shape is determined by minimization of the local isotropic bending energy [12] at given vesicle volume (V), membrane area (A) and difference between the areas of the two membrane lipid layers (ΔA)

$$\Delta A = h \int (C_1 + C_2) \mathrm{d}A. \qquad (1)$$

Here, h is the distance between the neutral surfaces of the outer and the inner membrane lipid layers, C_1 and C_2 are the principal membrane curvatures and $\mathrm{d}A$ is the infinitesimal membrane area element.

Within the bilayer couple model the vesicle shape depends on two geometrical parameters, i.e. the relative vesicle volume $v = (36\pi V^2/A^3)^{1/2}$ and the relative difference between the areas of the two membrane lipid layers $\Delta a = \Delta A/(16\pi A h^2)^{1/2}$ [7,11]. Both of these parameters are normalized relative to the corresponding values for the spherical cell that has the same membrane area. In accordance with the definition, the relative volume v and the relative area difference Δa of the spherical vesicle are equal to one [6,7]. A class of vesicle shapes is defined

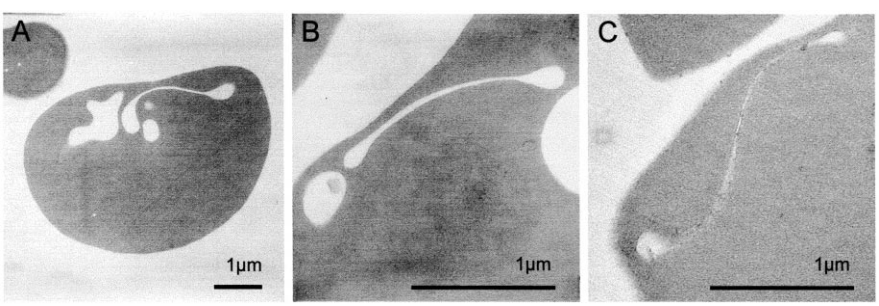

Fig. 2. Transmission electron micrographs of torocyte endovesicles of human erythrocytes incubated with C12E8 (adapted from Ref. [5]).

to contain all the stationary shapes of the same symmetry that can be continuously transformed into each other by continuously varying relative vesicle volume v and relative area difference Δa [8,13].

Fig. 3 shows a sequence of shapes corresponding to an increasing Δa within the torocyte–discocyte class of shapes. The shapes within this class have mirror symmetry with respect to the equatorial plane. The calculated shapes are obtained numerically by minimizing the local membrane bending energy at fixed A, V [6,14] and ΔA [7] as described in detail elsewhere [15,16]. In the case of the torocyte shapes (Fig. 3a,b), an additional constraint for the fixed (zero) distance between the opposing membranes along the circle bounding the flat central part of the torocyte is taken into account in the minimization procedure. It follows from the minimization procedure [14,16] that the principal curvature along the meridians is zero on this circle. There is a shape for $\Delta a = 1.0832$ (shape c in Fig. 3) where the two poles are touching each other. This shape represents the upper bound of the torocyte class and at the same time a lower bound of the discocyte class, i.e. below $\Delta a = 1.0832$ the vesicle shapes are torocytic while above $\Delta a = 1.0832$ the vesicle shapes are discocytic.

The possible region in the two-dimensional v–Δa phase diagram belonging to the class of the axisymmetrical torocyte vesicle shapes with equatorial mirror symmetry is shown in Fig. 4. The right boundary line represents discoidal shapes with two poles touching each other. The upper bound of discocyte class is the limiting shape resembling a shell composed of two equal sections of sphere (see Ref. [7] and references therein). At small Δa the region of the torocyte class is bounded by the shapes composed of a compressed plate-like central part and a toroidal periphery [17] (see also Fig. 7). For Δa lower than the boundary representing the limiting torocytes, there is a class of codocytes [6]. The class of codocytes partially overlaps with the class of torocytes.

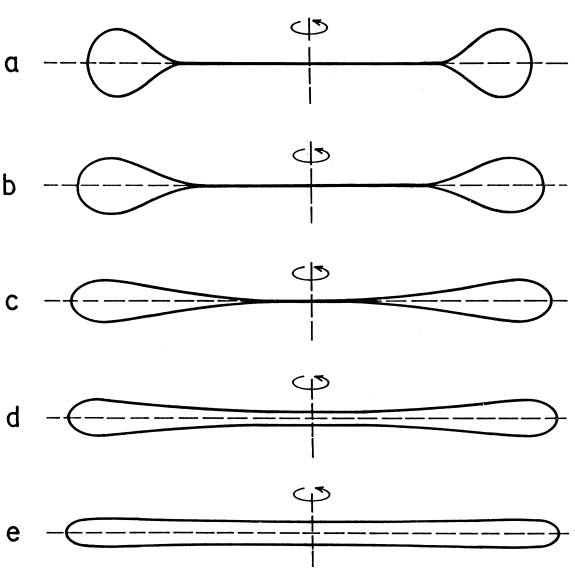

Fig. 3. Some characteristic shapes within the class of axisymmetric torocyte and discocyte oblate vesicles with equatorial mirror symmetry at relative vesicle volume $v = 0.2$ for different values of relative area difference Δa: (a) 1.0278, (b) 1.0608, (c) 1.0832, (d) 1.0896 and (e) 1.0960.

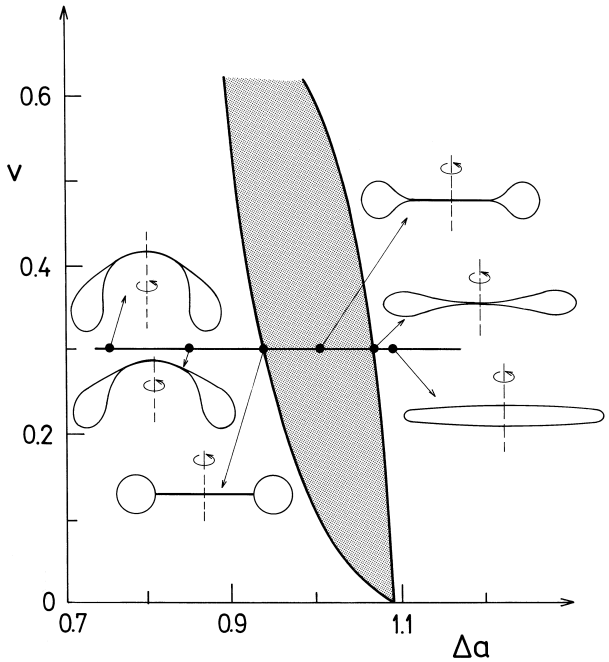

Fig. 4. Region in the $v-\Delta a$ phase diagram belonging to the class of the axisymmetrical torocyte vesicle shapes.

3. Molecular properties of C12E8-induced membrane inclusions and the stability of the observed torocyte endovesicles

3.1. Basic assumptions

Since intercalation of C12E8 (Fig. 1a) into the erythrocyte membrane induces inward membrane bending (stomatocytosis), we assume that C12E8 is preferentially located in the inner erythrocyte membrane layer [2], i.e. in the outer layer of the torocyte endovesicles. This is in agreement with the results of previous studies, which indicate a rapid flip-flop rate of C12E8 (in seconds) across the lipid bilayers [18,19]. By intercalating into the outer layer of the endovesicle membrane, the conical shaped C12E8 molecule [20] perturbs the membrane structure, e.g. causes a change in packing of the neighbour lipid molecules, partially also due to dehydration of their hydrophilic head groups [20–22]. As a consequence, C12E8-induced inclusion (cluster) is formed in the membrane [5,22], defined as a complex composed of the embedded C12E8 molecule and some adjacent phospholipid molecules which are significantly distorted due to the presence of the embedded C12E8 molecule. Since the acyl chains of the

individual phospholipid molecule in the neighborhood of C12E8 are moved apart sideways [21], the average acyl chain length of the phospholipid molecule shortens while its average area increases [23]. Consequently, the effective shape of the surrounding phospholipid molecules changes from a cylinder to an inverted truncated cone. Based on these experimental data, we take that the inclusion formed by the C12E8 molecule has the preference for small (zero) or even negative local membrane curvature [5,22].

3.2. Membrane free energy

To obtain the equilibrium shape of the vesicle at given external conditions, we should minimize the membrane free energy consisting of the contribution of the membrane continuum W and the contribution of the C12E8-induced membrane inclusions F_i:

$$F = W + F_i, \tag{2}$$

at given cell volume (V), membrane area (A) and area difference (ΔA).

For the contribution of the membrane continuum W we take the energy of the isotropic elasticity within the area-difference-elasticity model with spontaneous curvature (ADE-SC model) [13,24]. Within the ADE-SC model, the membrane elastic energy (W) which is the sum of the energy of the local isotropic bending (the first and second term) and the energy of the nonlocal isotropic bending (the third term) is

$$W = \frac{1}{2}k_c\int (C_1 + C_2)^2 \,\mathrm{d}A + k_G\int C_1C_2 \,\mathrm{d}A + \frac{k_r}{2Ah^2}(\Delta A - \Delta A_{ef})^2, \tag{3}$$

where k_c and k_G are the local and Gaussian bending moduli and k_r is nonlocal bending modulus [6,13,24,25]. The effective optimal area difference ΔA_{ef} is the sum of the area difference of the unstressed layers (ΔA_o) and the term proportional to the membrane spontaneous curvature (C_o) [24,26]

$$\Delta A_{ef} = \Delta A_o + \gamma C_o, \tag{4}$$

where γ is the constant which depends on the cell size and membrane properties. The experimentally determined value of ratio $k_r/k_c \cong 2$ [27].

The shear energy of the membrane skeleton [25,28,29] is neglected. Inclusion of the nonlocal bending energy (third term in Eq. (3)) in the minimization procedure does not change the calculated shapes at given ΔA. Only the energies of the obtained shapes are changed [13,15]. Consequently, the equilibrium value of ΔA at which the energy W (Eq. (3)) is at its minimum, is changed [26,30].

Phospholipid bilayers forming a closed surface and decorated with anisotropic inclusions that can orient in the plane of the membrane according to the local membrane curvature have been considered theoretically [31–33]. The orientation of the inclusion is given by the rotation of the principal directions of its intrinsic shape relative to the membrane principal directions (ω). The energy of the single inclusion expresses a mismatch between the intrinsic shape of the inclusion and the local membrane shape [33]:

$$E(\omega) = \xi\left(\overline{C} - \overline{C}_m\right)^2/2 + (\xi + \xi^*)\left(\hat{C}^2 - 2\hat{C}\hat{C}_m\cos(2\omega) + \hat{C}_m^2\right)/4, \tag{5}$$

where ξ and ξ^* are the constants representing the strength of the interaction between the inclusion and the membrane continuum, $\overline{C} = (C_1 + C_2)/2$ is the membrane mean curvature, $\hat{C} = (C_2 - C_1)/2$, $\overline{C}_m = (C_{1m} + C_{2m})/2$, $\hat{C}_m = (C_{2m} - C_{1m})/2$ and C_{1m} and C_{2m} are the principal curvatures of the intrinsic shape of the inclusion. If $C_{1m} = C_{2m}$, the inclusion is isotropic while if $C_{1m} \neq C_{2m}$, the inclusion is anisotropic, i.e. nonaxisymmetric with respect to the membrane normal vector.

According to statistical mechanics [34], the average orientation of the single anisotropic inclusion, described here by the average value of $\cos(2\omega)$, is

$$\langle\cos(2\omega)\rangle = \frac{\int_0^{2\pi}\cos(2\omega)\exp(-E(\omega)/kT)\,\mathrm{d}\omega}{\int_0^{2\pi}\exp(-E(\omega)/kT)\,\mathrm{d}\omega}, \tag{6}$$

where k is the Boltzmann constant and T is the temperature. The integration of the expressions in Eq. (6) gives the quotient of the modified Bessel functions I_0 and I_1

$$\langle\cos(2\omega)\rangle = \frac{I_1\left((\xi + \xi^*)\hat{C}\hat{C}_m/2kT\right)}{I_0\left((\xi + \xi^*)\hat{C}\hat{C}_m/2kT\right)}. \tag{7}$$

For illustration, Fig. 5 shows the average orientation of the anisotropic inclusion in dependence of the curvature

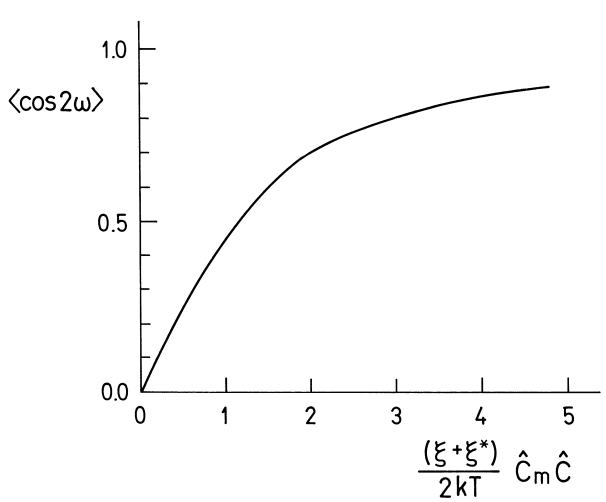

Fig. 5. The average orientation $\langle\cos(2\omega)\rangle$ of an anisotropic membrane inclusion in dependence of the local curvature deviator $\hat{C}$.

deviator ($\hat{C}$). It can be seen in Fig. 5 that the orientational ordering monotonously increases with increasing curvature deviator ($\hat{C}$).

The free energy of the inclusions F_i sharply decreases in the membrane regions with the favourable membrane mean curvature $\overline{C}$ and/or favourable curvature deviator $\hat{C}$ [33]. It has been shown recently that lateral distribution and local orientation of anisotropic inclusions may stabilize the narrow neck connecting the daughter vesicle and the mother cell [33].

The free energy of the inclusions in a given membrane layer can be written as [33]

$$F_i = -M_T\, kT \ln\left(\frac{1}{A}\int \exp\left(-\xi\left(\overline{C} \pm \overline{C}_m\right)^2/2kT - (\xi+\xi^*)\left(\hat{C}^2+\hat{C}_m^2\right)/4kT\right) \times I_0\left((\xi+\xi^*)\hat{C}\hat{C}_m/2kT\right)\mathrm{d}A\right), \quad (8)$$

where M_T is the total number of the inclusions in the layer and I_0 is the modified Bessel function obtained by the integration within the partition function of a single inclusion over all possible orientations [32]. The sign ($\pm$) denotes the choice of the inner/outer membrane area. The integration in Eq. (8) is performed over the entire membrane area.

As the free energy of the membrane inclusions depends on the shape and interactions of the C12E8 molecule, the vesicle shape would be determined in a specific manner. Currently, the model parameters ξ, ξ^*, C_{1m} and C_{2m} are not known for C12E8-induced inclusion so that we cannot make a definite prediction of how these molecules affect the vesicle shape. We can, however, indicate different possibilities that provide an explanation of the observed torocyte shape.

3.3. Preference of the C12E8-induced membrane inclusions for small or negative local curvature

The effective shape of the C12E8 membrane inclusion depends on the molecular shape of the intercalated C12E8 molecule and on its interaction with the surrounding lipids. Based on experimental data [20–23], it can be speculated that the effective shape of the membrane inclusion formed by the C12E8 molecule in the outer layer of the vesicle membrane can be characterized by small $\overline{C}_m$ with the preference for small local membrane curvature [22] or even negative $\overline{C}_m$ with the preference for negative local curvature [5]. The C12E8 membrane inclusions with $\overline{C}_m \cong 0$ [22] or slightly negative $\overline{C}_m$ [5] would favour the vesicle shape with large regions of small or negative mean curvature leading to torocyte vesicle shape (Figs. 2 and 3).

The influence of small or negative value of $\overline{C}_m$ of C12E8 inclusions on the vesicle shape can be described very illustratively in the limit of weak interaction between the C12E8 inclusion and the membrane, which leads to simple renormalization of the constants of the standard ADE-SC model. Namely, in this case the exponential and the logarithmic functions in Eq. (8) can be expanded. If further, at least one of the intrinsic curvatures of the inclusion C_{1m}, C_{2m} is much larger than any of the curvatures attained by the membrane C_1, C_2, the obtained free energy of the inclusions renormalizes the constants of the standard membrane elastic energy [31–33]. The corrected spontaneous curvature ($\overline{C}_o$) is [33]

$$\overline{C}_o \cong C_o + \frac{\xi M_T \overline{C}_m}{2Ak_c}. \quad (9)$$

If $\overline{C}_m$ of C12E8 membrane inclusions is small, the spontaneous curvature $\overline{C}_o$ very slowly increases with increasing number of intercalated C12E8 molecules while if $\overline{C}_m < 0$, the spontaneous curvature $\overline{C}_o$ decreases with increasing number of intercalated C12E8 molecules.

The optimal area difference of the endovesicle is increased mostly due to the preferential intercalation of the C12E8 molecules into the outer layer of the endovesicle, $\overline{\Delta A}_o = \Delta A_o + M_T A_{om}$, where A_{om} is the optimal area occupied by one C12E8 molecule. In the effective optimal area difference,

$$\Delta A_{ef} = \overline{\Delta A}_o + \gamma \overline{C}_o, \quad (10)$$

the effects of the spontaneous curvature may be small or even negative.

We propose that the above described effects of the C12E8-induced membrane inclusions on the effective optimal area difference ΔA_{ef} (Eq. (10)) causes that the shape of the extreme area difference within the given class of shapes [13,35] cannot be reached.

In contrast, some other stomatocytogenic amphiphiles [5,36] like chlorpromazine (Fig. 1b) and Triton X-100 (Fig. 1c) may increase the value of ΔA_{ef} of the endovesicles up to the maximal possible value within the given shape class. This may be achieved by intercalating preferentially into the inner layer of the erythrocyte membrane (outer layer of the endovesicle) and also by increasing the spontaneous curvature if the amphiphiles have the conical or truncated conical shape ($\overline{C}_m > 0$) [5]. For example, if erythrocytes are treated with sublytic concentrations of chlorpromazine, they reach the shape of extreme ΔA [13,35] composed of a spherical mother cell and many more or less spherical endovesicles [5].

To compare these two situations quantitatively, we made a simple calculation. For example, in the torocyte endovesicle with the relative volume $v = 0.2$, Δa is around 1.05 (Fig. 3). The value of Δa corresponding to 25 equivalent spherical endovesicles of the same enclosed total relative volume is together 5.0, i.e. approximately five times higher. We can see that the value of ΔA of the endovesicles obtained by chlorpromazine is much larger than of the corresponding ΔA of the torocyte endovesicle

induced by C12E8. We may conclude that C12E8 may induce the torocyte endovesicles due to small effect on ΔA_{ef} caused by the specific properties of the C12E8 inclusions.

If the interaction between the C12E8-induced membrane inclusion and the membrane is stronger the preference of the C12E8 inclusions for zero or negative local curvature may lead to nonhomogeneous lateral distribution of C12E8 inclusions [31,33]. Consequently, the C12E8 membrane inclusions could accumulate in the membrane of torocyte endovesicles.

3.4. Possible role of anisotropic properties of membrane inclusions in the stability of torocyte endovesicles

If the inclusions are anisotropic ($C_{1m} \neq C_{2m}$) and strongly interact with the membrane, the torocyte shape is additionally favoured. In the regions of the membrane where the difference between C_1 and C_2 is large the inclusions become orientationally ordered and the membrane exhibits deviatoric properties [32,33,37].

It can be shown that for large enough difference between the membrane principal curvatures C_1 and C_2 the contribution of the orientational ordering of the anisotropic inclusions to the free energy of the membrane can be expressed in the approximation of the constant area density of the inclusions up to a constant factor as

$$F_o = -kTm\int \ln\left(I_0\left((\xi+\xi^*)\hat{C}\hat{C}_m/2kT\right)\right)\mathrm{d}A, \qquad (11)$$

where $m = M_T/A$ is the area density of the inclusions and the integration is performed over the entire membrane area. In the case of $(\xi+\xi^*)|\hat{C}||\hat{C}_m|/2kT \geq 1$, the orientational contribution of the inclusions to the free energy of the membrane F_o (Eq. (11)) may be written as a linear function [38] of the integral of the curvature deviator D

$$F_o \cong -M_T(\xi+\xi^*)|\hat{C}_m|D/2A, \qquad (12)$$

$$D = \int |\hat{C}|\mathrm{d}A. \qquad (13)$$

The integration is performed over those parts of the membrane where the values of $(\xi+\xi^*)|\hat{C}||\hat{C}_m|/2kT \geq 1$. It can be seen from Eq. (12) that the orientational ordering of the inclusions lowers the membrane free energy.

Fig. 6 shows the calculated values of the integral of the curvature deviator D for the class of the axisymmetric torocyte endovesicle shapes with equatorial mirror plane symmetry given in Figs. 3 and 4. It can be seen in Fig. 6 that the integral of the curvature deviator of the torocyte vesicle continuously increases with decreasing relative area difference Δa of the torocyte vesicle which means that the orientational membrane free energy F_o (Eqs. (12) and (13)) is smaller for more pronounced torocytic shapes, i.e. for torocyte shapes with large central compressed region and small toroidal periphery. It can be, therefore, concluded that ordering of anisotropic membrane inclusions which orient as quadrupoles in the curvature field may additionally favour the formation of torocyte endovesicle shape.

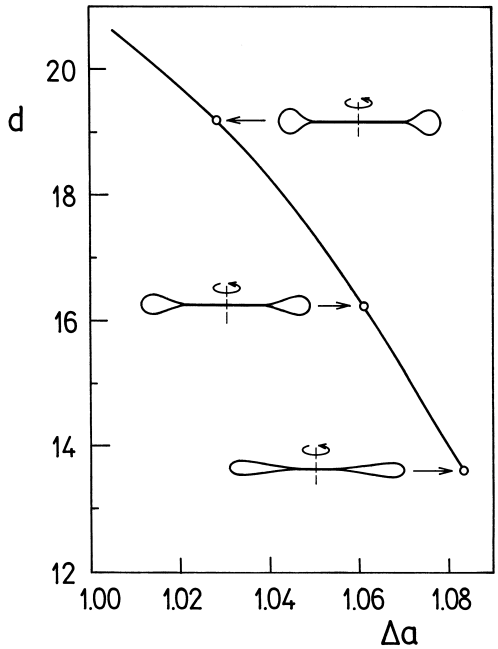

Fig. 6. The relative integral of the curvature deviator $d = D/(A/4\pi)^{1/2}$ of the axisymmetric torocyte vesicle shape (Fig. 3) as a function of the relative area difference Δa for the relative volume $v = 0.2$. The shapes presented are the same as some of the shapes presented in Fig. 3.

The minimization of the orientational free energy F_o (Eq. (12)) reduces to the problem of the extreme (maximal) integral of the curvature deviator (D) at fixed area (A) and fixed enclosed volume (V). For this purpose, a variational problem is stated by constructing a functional

$$G = D - \lambda_A\left(\int \mathrm{d}A - A\right) + \lambda_V\left(\int \mathrm{d}V - V\right), \qquad (14)$$

where λ_A and λ_V are the Lagrange multipliers and $\mathrm{d}V$ is the volume element.

The analysis is restricted to axisymmetric shapes. It is chosen that the symmetry axis of the body coincides with the x-axis, so that the shape is given by the rotation of the function $y(x)$ around the x-axis. In this case, the principal curvatures are expressed by $y(x)$ and its derivatives with respect to x: $y' = \mathrm{d}y/\mathrm{d}x$ and $y'' = \mathrm{d}^2y/\mathrm{d}x^2$ as

$$C_1 = \pm\left(1+y'^2\right)^{-1/2} y^{-1}, \qquad (15)$$

$$C_2 = \mp y''\left(1+y'^2\right)^{-3/2}. \qquad (16)$$

The area element is $\mathrm{d}A = 2\pi(1+y'^2)^{1/2}y\mathrm{d}x$, and the volume element is $\mathrm{d}V = \pm\pi y^2\mathrm{d}x$. By $(1\pm)$ it is taken into account that the function $y(x)$ may be multiple valued. The upper sign is taken for the convex regions and the lower sign is taken for the concave regions. The sign changes in the points where $y' \to \infty$.

The above expressions for C_1, C_2, $\mathrm{d}A$ and $\mathrm{d}V$ are inserted into Eq. (14) and rearranged to yield, $G = \pi \int g(x, y, y', y'')\mathrm{d}x$, where

$$g = |\mp 1 \mp yy''\left(1 + y'^2\right)| - 2\lambda_A y\left(1 + y'^2\right)^{1/2} \mp \lambda_V y^2. \quad (17)$$

The variation ($\delta G = 0$) is performed by solving the Euler–Poisson equation

$$\frac{\partial g}{\partial y} - \frac{\mathrm{d}}{\mathrm{d}x}\left(\frac{\partial g}{\partial y'}\right) + \frac{\mathrm{d}^2}{\mathrm{d}x^2}\left(\frac{\partial g}{\partial y''}\right) = 0. \quad (18)$$

The solutions of the variational problem are found by inserting different probe functions into Eq. (18). The system of circles of the radius $r_s: y = (r_s^2 - x^2)^{1/2}$ represents spheres or spherical sections with at most two different radii (r_{s1}, r_{s2}). For this solution $D = 0$ so that these shapes correspond to the absolute minimum of the average curvature deviator. Another solution is obtained by the constant $y = \lambda_A/\lambda_V$. This solution represents the cylinder. Further, the combination of functions

$$y = R + \left(r^2 - x^2\right)^{1/2} \quad (19)$$

and

$$y = R - \left(r^2 - x^2\right)^{1/2} \quad (20)$$

represents the torus or the limiting torocyte (Fig. 7).

All the above shapes of extreme D are characterized by two parameters, respectively, which can be determined from the constraints for the vesicle volume and area. As the number of the parameters equals the number of constraints, these shapes fulfill the requirement for the extreme [39]. The solutions representing torocyte shapes correspond to the observed endovesicle shapes that are the scope of this work.

At the present state of the knowledge about the geometrical structure of chlorpromazine and Triton X-100 in the lipid bilayer and the nature of their interactions with the adjacent phospholipid molecules it is impossible to make definite predictions about the ordering of chlorpromazine or Triton X-100 in the membrane.

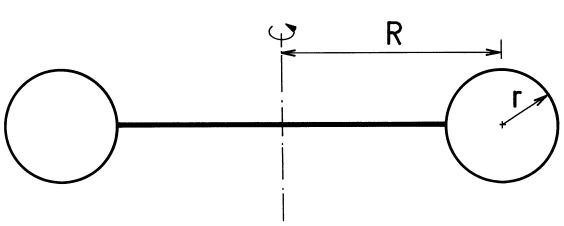

Fig. 7. Schematic presentation of the limiting torocyte composed of a plate-like central part of the radius R and a toroidal periphery of the radius r.

4. Discussion and conclusions

Recent experimental results show that C12E3 and C12E4 have no capacity to induce torocyte endovesicles (Hägerstrand et al., in preparation). The torocyte endovesicles can be observed only with homologues having five or more ethylene units. This correlates well with the latest results of Heerklotz et al. [22] which show that the cooperative interactions of C12En ($n = 3$–6) with a larger number of neighbouring lipid molecules (and consequent formation of detergent–lipid inclusion (cluster/raft) can be observed only for larger head-group detergents C12E5 and C12E6 and not for C12E3 and C12E4. Consequently, this strongly supports the idea that the creation of C12E8 membrane inclusion is essential for the formation of torocyte endovesicle.

Triton X-100, which induces small spherical endovesicles in erythrocytes, has similar hydrophilic head group as C12E8. However, while C12E8 bears a straight alkyl chain (Fig. 1a) Triton X-100 has a bulky hydrophobic part (Fig. 1c). This could be taken to indicate that both the hydrophilic and hydrophobic part of C12E8 may be essential in the capacity of C12E8 to induce the detergent–lipid inclusion.

It can be shown that the main relative radius of the limiting torocyte shape R increases while the relative radius r decreases with decreasing v. It can be also shown that the relative integral of the curvature deviator $d = D/(A/4\pi)^{1/2}$ of the limiting torocyte shape increases with decreasing relative vesicle volume v. Consequently, the enclosed relative volume of the limiting torocyte endovesicle should be as small as possible in order to render the relative integral of the curvature deviator d the largest. This agrees well with our experimental observations which show that the observed C12E8-induced torocyte endovesicle shapes (Fig. 2) have very small relative volume v.

The limiting torocyte shape (Fig. 7) is the shape of the extreme (maximal) integral of the curvature deviator D which can actually never be reached due to its very high (infinite) local bending energy but is however very close to the observed shapes (Fig. 2).

Since the absolute value of the curvature deviator $|\hat{C}|$ depends on the dimension of the vesicle, the energy F_o is not scale invariant as is the case in the local bending energy of the membrane [26]. Because the absolute value of F_o increases with decreasing dimensions of the vesicle the approximative expression for F_o (Eqs. (12) and (13)) can be used only for highly curved vesicles [38] where the values of $|\hat{C}|$ are large enough. In the case of limiting torocyte vesicles (Fig. 7), the orientational contribution to the free energy of the membrane (F_o) may be considerable only for small r. It can be seen in Fig. 2 that the radius of the bulby end of the observed torocyte endovesicle is indeed very small. Consequently, the curvature deviator $|\hat{C}|$ as well as the orientational energy F_o of these regions may be considerably large (and negative).

A problem related to the formation of the torocyte endovesicles and concerning cylindrical structures has recently been considered. Stable cylindrical structures composed of the phospholipid and geraniol were observed [38,40,41]. Geraniol molecules are dimeric amphiphiles and therefore highly anistropic [40,41]. It has been suggested [32,33,38,41,42] that the stable cylindrical structures could not be predicted within the standard membrane elastic energy models and that the deviatoric properties of the membrane may provide a plausible explanation for the observed shapes. Further, also in erythrocytes, stable cylindrical microexovesicles were observed [28,36,38]. Mainly cylindrical microexovesicles were observed upon adding the anisotropic amphiphile dodecyl maltoside (which has a bulky dimeric polar head) and an anisotropic dimeric cationic amphiphile to the erythrocyte suspension [38].

Regarding the ADE-SC model [13,24], it should be stressed that this model is the limiting case of the more general models which take into account the nonhomogeneous lateral distribution of the membrane constituents [31,33,43–45]. It has been shown in many studies that standard ADE-SC model itself cannot account for some of the observed phenomena in the liposome physics as well as in the physics of erythrocytes. For example, it cannot describe completely the observed budding transions in phospholipid vesicles [33,46] or explain the stability of tubular structures/vesicles [33,38,41,42]. Furthermore, in the case of erythrocyte, the shear energy of the skeleton, the skeleton–bilayer interactions and some other interactions in the membrane should be taken into account to fit adequately the experimental results [30,47–52]. To conclude, the ADE-SC model can explain many of the observed phenomena, however, in some cases including the one considered in this work the ADE-SC model should be upgraded.

The above theoretical predictions and the fact that we occasionally observed cylindrical endovesicles in addition to the torocyte endovesicles upon adding C12E8 to the erythrocyte suspension, indicate that the deviatoric properties of the membrane and a nonhomogeneous lateral distribution of the C12E8 inclusions might contribute to the stabilization of nonspherical erythrocyte daughter vesicles [33,38]. However, definite answers regarding the strength and the nature of the interaction between the inclusion and the membrane could not be given without additional experimental results.

We show that due to the possible orientational ordering of the phospholipid molecules within the C12E8–lipid complexes (inclusions) in the toroidal regions of the erythrocyte membrane the torocyte endovesicle shapes with very small relative volume v are favoured in order to have a large integral of the curvature deviator D, and consequently, the smallest orientational free energy F_o (Eq. (12)).

Since membrane intercalation of C12E8 induces stomatocytosis and because the C12E8 membrane inclusion seems to be characterized by small ($\overline{C}_m \cong 0$) or slightly negative value of $\overline{C}_m$ we assumed on the basis of Eqs. (9) and (10) that C12E8 is preferentially located in the inner erythrocyte lipid layer [5]. However, if the $\overline{C}_m$ value of C12E8 inclusions would be strongly negative ($\overline{C}_m \ll 0$) it would be also possible (see Eqs. (9) and (10)) that C12E8 is preferentially located in the outer lipid layer of erythrocyte membrane (see also Ref. [53]).

In conclusion, we suggest that the stable torocyte endovesicle shape may be explained by three partly complementary mechanisms: by the preferential intercalation of the C12E8 molecules into the inner membrane layer, by the preference of the C12E8-induced membrane inclusions for small or slightly negative local curvature which may lead also to the nonhomogeneous lateral distribution of the C12E8 inclusions and by the orientational ordering of the C12E8 molecules in the regions of high local membrane curvature deviator.

Acknowledgements

We are indebted to Esa Nummelin for help with preparing the figures. We are also indebted to Research Institute and the Rector at the Åbo Akademi University and to Ministry of Science and Technology of the Republic of Slovenia for their financial support.

References

[1] B. Deuticke, Transformation and restoration of biconcave shape of human erythrocytes induced by amphiphilic agents and changes of ionic environment, Biochim. Biophys. Acta 163 (1968) 494–500.
[2] M.P. Sheetz, S.J. Singer, Biological membranes as bilayer couples. A molecular mechanism of drug–erythrocyte interactions, Proc. Natl. Acad. Sci. 71 (1974) 4457–4461.
[3] H. Hägerstrand, B. Isomaa, Lipid and protein composition of exovesicles released from human erythrocyte following treatment with amphiphiles, Biochim. Biophys. Acta 1190 (1994) 409–415.
[4] B. Deuticke, R. Grebe, C.W.M. Haest, Action of drugs on the erythrocyte membrane, in: J.R. Harris (Ed.), Erythroid Cells, Plenum, New York, 1990, pp. 475–529.
[5] M. Bobrowska-Hägerstrand, V. Kralj-Iglič, A. Iglič, K. Bialkowska, B. Isomaa, H. Hägerstrand, Torocyte membrane endovesicles induced by octaethyleneglycol dodecylether in human erythrocytes, Biophys. J. 77 (1999) 3356–3362.
[6] H.J. Deuling, W. Helfrich, The curvature elasticity of fluid membranes, J. Phys. (France) 37 (1976) 1335–1345.
[7] S. Svetina, B. Žekš, Bilayer couple as a possible mechanism of biological shape formation, Biochim. Biophys. Acta 44 (1985) 979–986.
[8] U. Seifert, K. Berndl, R. Lipowsky, Shape transformations of vesicles: phase diagram for spontaneous-curvature and bilayer-coupling models, Phys. Rev. E 44 (1991) 1182–1202.
[9] R. Lipowsky, The conformation of membranes, Nature 349 (1991) 475–481.
[10] E.A. Evans, Bending resistance and chemically induced moments in membrane bilayers, Biophys. J. 14 (1974) 923–931.
[11] V. Kralj-Iglič, S. Svetina, B. Žekš, The existence of non-axisymmetric bilayer vesicle shapes predicted by the bilayer couple model, Eur. Biophys. J. 22 (1993) 97–103.

[12] W. Helfrich, Blocked lipid exchanges in bilayers and its possible influence on the shape of vesicles, Z. Naturforsch. 29c (1974) 510–515.
[13] S. Svetina, A. Iglič, B. Žekš, On the role of the elastic properties of closed lamellar membranes in membrane fusion, Ann. N. Y. Acad. Sci. 416 (1994) 179–191.
[14] F. Jülicher, U. Seifert, Shape equations for axisymmetrical vesicles: a clarification, Phys. Rev. E 49 (1994) 4728–4731.
[15] V. Heinrich, Theoretische Bestimmung von kugelnahen Vesikelformen mit Hilfe von Kugelfunktionen, Thesis, Humboldt University, Berlin, Germany, 1991.
[16] B. Božič, S. Svetina, B. Žekš, Theoretical analysis of the formation of membrane microtubes on axially strained vesicles, Phys. Rev. E 55 (1997) 5834–5842.
[17] H. Hägerstrand, V. Kralj-Iglič, M. Bobrowska-Hägerstrand, K. Bialkowska, B. Isomaa, A. Iglič, Torocytes — a new class of vesicle shapes, Cell. Mol. Biol. Lett. 3 (1998) 145–150.
[18] U. Kragh-Hansen, M. le Maire, J.V. Moller, The mechanism of detergent solubilization of liposomes and protein-containing membranes, Biophys. J. 75 (1998) 2932–2946.
[19] M. Maire, J.V. Moller, P. Champeil, Binding of a nonionic detergent to membranes: flip-flop rate and location on the bilayer, Biochemistry 26 (1987) 4803–4810.
[20] H. Heerklotz, H. Binder, G. Lantzsch, G. Klose, A. Blume, Lipid/detergent interaction thermodynamics as a function of molecular shape, J. Phys. Chem. B 101 (1997) 639–645.
[21] R.L. Thurmond, D. Otten, M.F. Brown, K. Beyer, Structure and packing of phosphatidylcholines in lamellar and hexagonal liquid–crystalline mixtures with a nonionic detergent: a wide-line deuterium and phosphorus-31 NMR study, J. Phys. Chem. 98 (1994) 972–983.
[22] H. Heerklotz, H. Binder, H. Schmiedel, Excess-enthalpies of mixing in phospholipid-additive membranes, J. Phys. Chem. B 102 (1998) 5363–5368.
[23] D. Otten, L. Löbbecke, K. Beyer, Stages of the bilayer-micelle transition in the system phosphatidylcholine–C12E8 as studied by deuterium and phosphorus NMR, light scattering, and calorimerty, Biophys. J. 68 (1995) 584–597.
[24] L. Miao, U. Seifert, M. Wortis, H.G. Döbereiner, Budding transitions of fluid-bilayer vesicles; the effect of area difference elasticity, Phys. Rev. E 49 (1994) 5389–5407.
[25] E. Evans, R. Skalak, Mechanics and Thermodynamics of Biomembranes, CRC Press, Boca Raton, FL, 1980.
[26] U. Seifert, Configurations of fluid membranes and vesicles, Adv. Phys. 46 (1997) 13–137.
[27] W.C. Hwang, R.E. Waugh, Energy of dissociation of lipid bilayer from the membrane skeleton of red blood cells, Biophys. J. 72 (1997) 2669–2678.
[28] H. Hägerstrand, V. Kralj-Iglič, M. Bobrowska-Hägerstrand, A. Iglič, Membrane skeleton detachment in spherical and cylindrical microexovesicles, Bull. Math. Biol. 61 (1999) 1019–1030.
[29] A. Iglič, V. Kralj-Iglič, H. Hägerstrand, Stability of spiculated red blood cells induced by intercalation of amphiphiles in cell membrane, Med. Biol. Eng. Comput. 36 (1998) 251–255.
[30] A. Iglič, V. Kralj-Iglič, H. Hägerstrand, Amphiphile induced echinocyte–spheroechinocyte red blood cell shape transformation, Eur. Biophys. J. 27 (1998) 335–339.
[31] V. Kralj-Iglič, S. Svetina, B. Žekš, Shapes of bilayer vesicles with membrane embedded molecules, Eur. Biophys. J. 24 (1996) 311–321.
[32] J.B. Fournier, Nontopological saddle-splay and curvature instabilities from anisotropic membrane inclusions, Phys. Rev. Lett. 76 (1996) 4436–4439.
[33] V. Kralj-Iglič, V. Heinrich, S. Svetina, B. Žekš, Free energy of closed membrane with anisotropic inclusions, Eur. Phys. J. B 10 (1999) 5–8.
[34] T.R. Hill, An Introduction to Statistical Thermodynamics, Dover Publications, New York, 1986.
[35] A. Iglič, H. Hägerstrand, V. Kralj-Iglič, M. Bobrowska-Hägerstrand, A possible physical mechanism of red blood cell vesiculation obtained by incubation at high pH, J. Biomechanics 31 (1998) 151–156.
[36] H. Hägerstrand, B. Isomaa, Morphological characterization of exovesicles and endovesicles released from human erythrocytes following treatment with amphiphiles, Biochim. Biophys. Acta 1109 (1992) 117–126.
[37] T.M. Fischer, Bending stiffness of lipid bilayers: V. Comparison of two formulations, J. Phys. II (Paris) 3 (1993) 1795–1805.
[38] V. Kralj-Iglič, A. Iglič, H. Hägerstrand, P. Peterlin, Stable tubular microexovesicles of the erythrocyte membrane induced by dimeric amphiphiles, Phys. Rev. E 61 (2000) 4230–4234.
[39] L.E. Elsgolc, Calculus of Variations, Pergamon, Oxford, 1963.
[40] S. Chiruvolu, H.E. Warriner, E. Naranjo, S.H.J. Idziak, J.O. Rädler, R.O. Plano, J.A. Zasadzinski, C.R. Safinya, A phase of liposomes with entangled tubular vesicles, Science 266 (1994) 1222–1225.
[41] C.R. Safinya, Biomolecular materials: structure, interactions and higher order self-assembly, Coll. Surf. A 128 (1997) 183–195.
[42] J.B. Fournier, P. Galatola, Tubular vesicles and effective fourth-order membrane elastic theories, Europhys. Lett. 39 (1997) 225–230.
[43] S. Leibler, Curvature instability in membranes, J. Phys. 47 (1986) 507–516.
[44] U. Seifert, Curvature-induced lateral phase segregation in two-component vesicles, Phys. Rev. Lett. 70 (1993) 1335–1338.
[45] D. Andelman, T. Kawakatsu, K. Kawasaki, Equilibrium shape of two-component unilamellar membranes and vesicles, Europhys. Lett. 19 (1992) 57–62.
[46] J. Käs, E. Sackmann, Shape transitions and shape stability of giant phospholipid vesicles in pure water induced by area-to-volume changes, Biophys. J. 60 (1991) 825–844.
[47] A. Elgsaeter, B.T. Stokke, A. Mikkelsen, D. Branton, The molecular basis of erythrocyte shape, Science 234 (1986) 1217–1223.
[48] J. Gimsa, C. Ried, Do band 3 protein conformational changes mediate shape changes of human erythrocytes, Mol. Membr. Biol. 12 (1995) 247–254.
[49] T. Hianik, V. Passechnik, Bilayer Lipid Membranes: Structure and Mechanical Properties, Kluwer Academic Publishing, Dordrecht, 1995.
[50] R.E. Waugh, Elastic energy of curvature-driven bump formation on red blood cell membrane, Biophys. J. 70 (1996) 1027–1035.
[51] M. Bobrowska-Hägerstrand, H. Hägerstrand, A. Iglič, Membrane skeleton and red blood cell vesiculation at low pH, Biochim. Biophys. Acta 1371 (1998) 123–128.
[52] A.A. Boulbitch, Deflection of a cell membrane under application of local force, Phys. Rev. E 57 (1998) 1–5.
[53] B. Roelofsen, F.A. Kuypers, J.A.F. Op den Kamp, L.L.M. van Deenen, Influence of phosphatidylcholine molecular species composition on the stability of erythrocyte membrane, Biochem. Soc. Trans. 17 (1989) 284–286.